Biochimica et Biophysica Acta, 1149 (1993) 119–126

BBAMEM 75997

Membrane changes accompanying the induced differentiation of Friend murine erythroleukemia cells studied by dielectrophoresis

Peter R.C. Gascoyne [a], Ronald Pethig [b], Julian P.H. Burt [b] and Frederick F. Becker [a]

[a] *Department of Molecular Pathology, University of Texas M.D. Anderson Cancer Center, Houston, TX (USA) and* [b] *Institute of Molecular and Biomolecular Electronics, University of Wales, Bangor (UK)*

(Received 28 December 1992)

Key words: Dielectrophoresis; Cell surface; Membrane conductivity; Surface charge; (Friend erythroleukemia cell)

Dielectrophoresis measurements obtained using an image processing technique are reported over the frequency range 1 Hz to 100 kHz for the Friend murine erythroleukemia cell lines DS19 and R1 before and after treatment with hexamethylene bisacetamide and dimethylsulfoxide, agents that induce terminal differentiation in DS19 but not in R1 cells. Data are analyzed according to the single shell dielectric model of the cell. The membrane capacitance was found to fall by 30% and membrane conductivity by a factor of at least 5 when DS19 cells were induced to differentiate. R1 cells showed no such response. While the theoretical model was found to be useful for comparing differences in data for the different cell lines, several significant discrepancies between its predictions and the experimental data were observed, including positive dielectrophoretic collection at frequencies below 20 Hz and a smaller than predicted response to the membrane permeabilizing agents saponin and valinomycin. Factors that may have accounted for these discrepancies include surface charge effects, conduction parallel to the plasma membrane surface, and intracellular compartments.

Introduction

The phenomenon of dielectrophoresis (DEP) has been exploited for the investigation of viable bacterial, plant and mammalian cells [1–7]. In these studies, cells are exposed to an inhomogeneous electric field and differences in their electrical polarizability with respect to the suspending medium become manifest as translational forces. Measurement of motion induced by these forces at different frequencies of the applied field allows the frequency-dependence of the polarizability of the cells relative to their surroundings to be deduced [8]. By using an optical absorbance technique to measure the dielectrophoretic collection of cells on an interdigitated electrode array, we showed previously that the DEP properties of three cultured Friend murine erythroleukemia cell lines changed following treatment with the differentiation-inducing agent hexamethylene bisacetamide (HMBA) [4]. Each of the three lines was chosen because it exhibited a unique differentiation response to HMBA as judged by phenotypic alterations and loss of cloning efficiency on soft agar plates [9–14]. Changes in the DEP characteristics of each line following HMBA treatment closely paralleled the extent of the differentiation response, suggesting that the dielectrophoretic characteristics could be used to analyze cellular responses to this differentiating agent.

More recently, we have developed an image-processing technique to allow a more complete analysis of the DEP motion of cells [15,16] and have shown that collection at the electrodes can occur not only by positive but also by negative DEP [15,17], a finding that was not taken into account in our earlier light absorbance measurements, which determined the magnitude, but not the sign, of the cell collection. In this paper, we reexamine two of the erythroleukemia cell lines using the image-processing technique and extend our DEP observations. We report the effects of enzymatic cleavage of sialic acid (which reduces net cell surface charge) and of ionophoric and ion-channel blocking techniques (which alter the ionic conductivity of the plasma membrane) on the DEP collection spectra of the cells. The observed responses are compared with predictions of the single-shell dielectric model of the cell [18]. We demonstrate that the observed DEP responses exhibit several anomalies with respect to the predictions of the single-shell model. Discrepancies include a smaller response than expected to ionophores

Correspondence to: P.R.C. Gascoyne, Department of Molecular Pathology, Box 89, University of Texas M.D. Anderson Cancer Center, 1515 Holcombe Boulevard, Houston, TX 77030, USA.

and an anomalous positive DEP response at low frequencies (below 20 Hz). The low-frequency anomaly [4,8], which was reported earlier by Kaler et al. to occur also in Canola plant cells [7,19], is discussed in terms of cell surface charge and time-dependent ion-channel gating. Cell surface charge, internal compartmentalization of ions, and distinct conductance components along and through the membrane surface are factors that appear to be important to the DEP behavior of viable erythroleukemia cells.

Materials and Methods

Cells of Friend murine erythroleukemia lines DS19 and R1 were seeded at 10^5 cells/ml and grown in 300 ml of minimum essential medium (MEM) supplemented with 10% fetal bovine serum, 1 mM glutamine, 1 μg/ml gentamicin, 2 mg/ml dextrose, and 20 mM Hepes buffer in suspension bottles at 37°C under a 5% CO_2/95% air atmosphere. Cultures were rotated at 0.5 rev/min in a Bellco roller bottle cell production incubator for 2 days, at which time cell density had reached about $1.5 \cdot 10^6$ cells/ml with at least 95% viability.

In differentiation treatments, 4 mM hexamethylene bisacetamide (HMBA, Sigma, St. Louis, MO) was added to the culture medium during seeding. After 2 days of treatment, the cells were reseeded at 10^5 cells/ml into fresh medium again containing 4 mM HMBA and grown for two more days. In this way, cells were exposed to HMBA for an optimum 4-day differentiation treatment, while the culture density and length of time since refeeding was the same at harvest as for untreated cell cultures.

Cells were harvested by centrifugation at $600 \times g$ for 10 min, washed twice in 320 mM sucrose supplemented with 3 mg/ml dextrose, resuspended in this solution at a density of 10^7/ml, and examined immediately by DEP. When several DEP spectra were to be taken, only part of the culture was harvested; fresh aliquots of cells were harvested and washed for each spectrum.

For each DEP determination, cells suspended in sucrose solution were injected into a DEP chamber [15] and allowed to settle for 90 seconds onto an interdigitated electrode array. Cell motion induced by an inhomogeneous electrical field generated by the electrode array, and having a maximum strength of $3 \cdot 10^5$ V/m, was then determined by an automatic image-processing technique in which the net motion of cells into positive and negative DEP collection regions was measured [15,16]. DEP collection spectra were measured over the range 1 to 100 kHz at five points per decade with three replicate samples per point. In specific instances where the effects of modifiers of cell membrane characteristics were being studied, frequencies as low as 1 Hz were used. A fresh sample aliquot was injected onto the electrode array and allowed to settle before every point.

K^+ concentrations were measured with an Orion 920A computing ion analyzer equipped with a K^+-sensitive electrode. A three-point calibration method was utilized in which known concentrations of K^+ were dissolved in the sucrose solution in the absence of cells and the corresponding electrode potentials were stored in the instrument which then read out K^+ concentrations directly. Leakage of K^+ from cells was determined by suspending $2 \cdot 10^7$ cells/ml in 20 ml of the sucrose solution and then measuring the concentration of K^+ that in the extracellular space as a function of time for up to 90 min following suspension of the cells. At that time, 40 μg/ml saponin was added to the mixture, a concentration known to rapidly permeabilize the cell plasma membrane [20], and the K^+ concentration was determined after an additional 60 min. The sample was then sonicated to break up the cells and release the enclosed ions, after which the total cellular content of K^+ was measured. Electrode calibration was checked with a standard after each measurement step and, in order to ensure that the sensitivity of the electrode was not altered in the presence of components in the saponin/cell debris mixture, the expected response to known additions of K^+ was confirmed with the electrode sitting in this mixture.

Ionic leakage from the cells was also observed by measuring the conductivity of the extracellular space. An identical cell suspension to that used in K^+ experiments was measured using a Cole-Parmer 19101-00 specific conductance meter equipped with temperature compensation over the same time-course and with the same saponification and sonication treatments at the end. The conductivity probe was placed in the cell mixture every 10 to 20 min for just long enough to obtain a stable reading and then removed immediately to avoid damage to the cells.

The conductivity of each sample was measured immediately after it flowed out of the DEP chamber during changing by using the same specific conductance instrument equipped with a flow microcell and temperature compensation. The typical conductivity of a fresh sample containing 10^7 cells/ml was 2 mS/m; this increased slowly with time because of ionic leakage from the cells (see below). Because of this, it was impractical to measure complete DEP collection spectra (each involving 32 sample changes) at one controlled conductivity. Instead, both the DEP collection rate and the sample conductivity were recorded simultaneously as the frequency response was investigated. DEP spectra and their accompanying conductivity data were collected for individually washed sample aliquots (all derived from a single roller bottle culture) adjusted with a few microliters of 0.1 M KCl to starting conductivities of approximately 2, 4, 6 and 8 mS/m, respec-

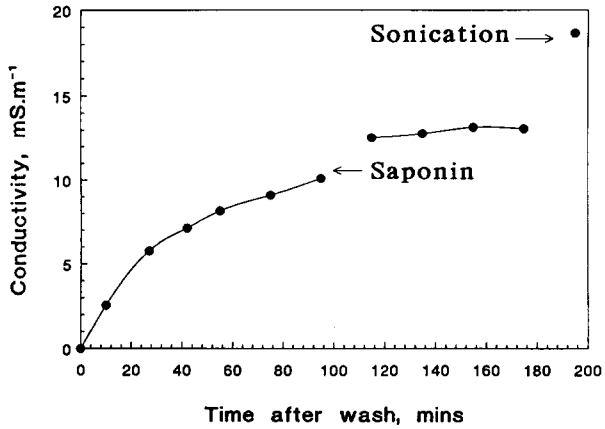

Fig. 1. Increase of conductivity of a suspension of 10^7 cells/ml in 320 mM sucrose-3 mg/ml dextrose solution. Following sonication of the cells, the ionic conductivity of the medium increased substantially, indicating that not all ions leaked from the intact cells in sucrose suspension.

tively. Such sets of four spectra were measured in at least five repeats of the experiment made on different occasions using identical cell culture conditions.

Results

Ionic determinations

The conductivity of sample suspensions increased with time following washing and resuspension in 320 mM sucrose solution as ions slowly leaked from the cells (Fig. 1). Ion-sensitive electrode measurements showed that the predominant cation involved in this leakage was K^+, which accounted for at least 90% of the cationic flux. The initial rate of ionic leakage depended upon the phase of growth at which cell cultures were harvested. The cells of mid-log phase cultures having a density of 10^6 cells/ml, for example, demonstrated conductivity that initially increased at a rate of approximately 1.5 μS/m per s. When cultures were in the plateau phase (approx. $3.5 \cdot 10^6$ cells/ml), the initial rate of ion leakage in samples tripled (4.6 μS/m per s). Following 3 days of differentiation treatment with HMBA, the rate of ion leakage of mid-log-phase cells decreased to about 0.5 μS/m per s.

DEP measurements

Spectra were plotted as 3-D surfaces of DEP collection rate vs. frequency and conductivity. Fig. 2 shows the combined data for 10 separate runs on DS19 harvested at mid-log phase with no differentiation treatment. A gridding algorithm was used to generate a plane from the combined set of data triplets. Part of the plane corresponding to a DEP collection rate of zero is also shown in this 3-D plot. Above this plane DEP values are positive and correspond to cell movement towards regions on the electrode array of high E^2, while DEP values below are negative and indicate motion away from such regions (see Discussion). Intersection of the two planes indicates the locus of conditions under which no net cell motion occurs, leading to a cross-over in the sign of the DEP rate. This locus is shown projected against the Frequency vs. Conductivity axis of Fig. 2. Similar 3-D plots were obtained for DS19 and R1 cells following treatment with HMBA and loci of cross-over points for both the untreated and treated

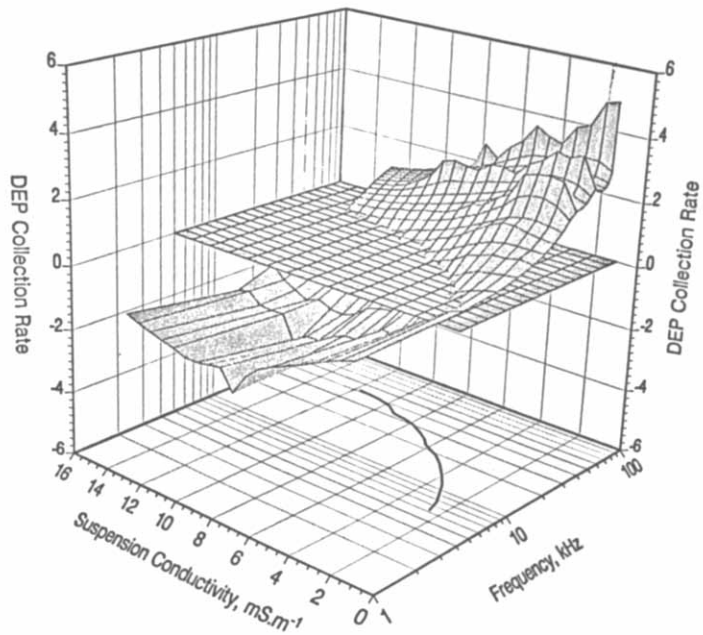

Fig. 2. Typical dielectrophoretic collection surface obtained by using a gridding algorithm to smooth 10 separate sets of data. The data shown are for DS19 without HMBA treatment. The plane corresponding to zero DEP collection is also shown. The intersection of this plane with the DEP collection surface indicates the locus of conditions where DEP motion was zero. The rate of cell collection is plotted in arbitrary units.

DS19 samples are shown plotted on linear axes in Fig. 3. At a given suspension conductivity, the cross-over frequency for HMBA-treated DS19 cells can be seen from this graph to be always higher than the corresponding cross-over frequency for untreated cells. Furthermore, the intercept on the conductivity axis is smaller for treated than for untreated cells. Thus, DS19 cells responded to differentiation treatment in a manner detectable by DEP. On the other hand, the response of R1 to HMBA treatment was minimal (data not shown).

In our previously reported dielectrophoretic measurements using the optical absorbance method, we observed strong collection of DS19 cells below 15 Hz. Since the optical absorbance method was unable to distinguish between positive and negative dielectrophoretic collection, we reexamined dielectrophoresis of DS19 in this frequency range using the image analysis method. Because the net surface charge of the cells caused an oscillatory electrophoretic motion at frequencies below about 50 Hz, a modified image-analysis technique was employed. Instead of measuring the cell motion as a function of time and computing the collection rate, a single determination was made of the total change in cell distribution after a 20-s application of the electric field, a period over which net cell motion greatly exceeded the electrophoretically-induced oscillatory excursions. At a frequency of 20 Hz, no net motion occurred for untreated DS19 cells. Below this frequency, however, cells exhibited a positive dielectrophoretic collection, the extent of which increased with decreasing frequency (see Fig. 4).

Cell surface modifications

Treatment of the cells with 10 U/ml neuraminidase for 30 min at 37°C significantly lowered the low-

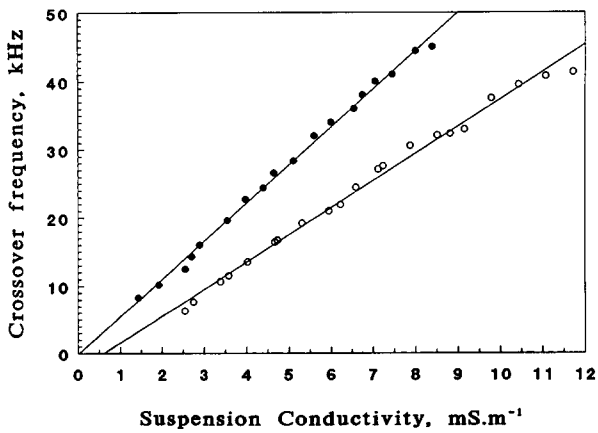

Fig. 3. Dependence of the cross-over frequency, at which the dielectrophoretic force on the cells is zero, on the cell suspension conductivity for DS19 cells before (○) and after (●) treatment with HMBA for 4 days. These responses represent linearized versions of the intersections of the DEP collection surfaces and the plane of zero DEP motion as illustrated in Fig. 2.

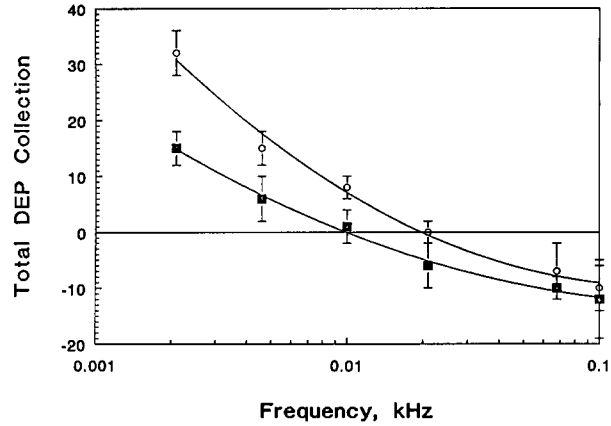

Fig. 4. Low-frequency DEP collection of DS19 cells. A positive collection is not expected with falling frequency from current theoretical models describing DEP [24]. Untreated cells (○) exhibited a stronger positive collection response than cells treated with neuraminidase to reduce their net surface charge by approx. 60% (■). The bars show the standard deviation of three measurements.

frequency positive DEP collection and dropped the cross-over frequency to 10 Hz. Electrophoretic measurements using the method previously reported from this laboratory [14] showed that the net surface charge fell by 60% as a result of treatment with neuraminidase. The dielectrophoretic properties of the cells were found to be unchanged in the frequency range 2 kHz to 100 kHz by neuraminidase treatment, however, indicating that the influence of net cell surface charge on DEP responses is limited to the low-frequency region.

In another manipulation of cell membrane properties, HMBA-treated cells were exposed to saponin or valinomycin in order to alter ion leakage from the membrane. Cells treated with 12 $\mu g/ml^{-1}$ saponin or 1 μM valinomycin exhibited almost unchanged DEP responses for the first 20 minutes. Thereafter dielectrophoretic collection at 100 kHz fell off, suggesting that it took some time for the conductivity of intracellular spaces to approach that of the suspending medium following treatment with the permeabilizing agents.

Discussion

Dielectrophoresis is an effect that depends upon the difference between the electrical polarizability of a particle and and that of its surroundings and upon the inhomogeneity of the applied electrical field. The phenomenological equation describing the effect is given in Appendix A, and indicates that the DEP force will be directed towards strongly inhomogeneous regions of the electric field when a particle is more electrically polarizable than its surroundings and, conversely, away from such field regions when it is less polarizable. Motion towards highly inhomogeneous field regions is

termed positive DEP; motion away is termed negative DEP. Because the electrical polarizability depends on the frequency of the applied electrical field, there are some frequencies bands where positive DEP occurs and others where the DEP motion is negative. For example, at frequencies around 1 kHz, the insulating properties of the plasma membrane of cells acted as an effective barrier to the applied electrical field and the cells behaved like non-conductive particles suspended in a more conductive medium. As a result, they experienced negative DEP. At 100 kHz, however, the capacitance of the cell membranes coupled the electrical field into the cytoplasms so that, from an electrical standpoint, cell plasma membranes became completely invisible. Because the cells were washed in a manner that kept most of the ions trapped inside while removing most ions from the suspending medium, they then appeared like electrically conductive balls in a weakly-conductive medium and experienced strongly positive DEP.

Dielectrophoretic measurements using the optical absorbance method over the frequency range 1 Hz–10 MHz were reported by us previously for DS19, R1 and DR10 cells. Here we have reexamined the 1 Hz to 100 kHz frequency range using an image-processing technique that allows spectra to be determined automatically while taking into account the subtleties of the DEP motion to different regions of the electrode array. DEP motion was positive not only at frequencies above 50 kHz, but also at frequencies below 20 Hz. Negative DEP motion occurred in the frequency range 20 Hz to 10 kHz. That active collection at the electrode array, rather than gentle repulsion from the array, could be caused by negative DEP effects was a subtlety not recognized in our earlier paper, which showed spectra of the magnitude, but not the phase, of the DEP collection of the MEL cells. Pictures showing the resulting collection patterns have been reported by us earlier [17].

Various models have been proposed to allow specific cellular characteristics to be extracted from the DEP spectra such as the multi-shell model derived by Irimajiri et al. [21], which considers the cell to consist of a set of homogeneous spherical shells. For our mammalian cells, this can, as a first approximation, be simplified to a single shell (representing the cytoplasm) surrounded by a thin, homogeneous, spherical membrane. The corresponding mathematical expression for the effective permittivity of the cell can then be written in the form shown in Appendix A. Analysis of the DEP data according to this approximation then allows values to be derived for the electrical permittivity and conductivity of the membrane and cytoplasm (denoted by ϵ_{mem} and σ_{mem}, and by ϵ_{in} and σ_{in}, respectively), if the corresponding properties of the suspending medium are known.

Multi-shelled models introduce more dielectric and conduction parameters but, in the absence of more refined data on the structure of the cell, these introduce additional degrees of freedom of doubtful physical significance when curve fitting the DEP data. The single-shell model permits us to interpret results in terms of dielectric and conduction effects of the membrane and cytosol only and ignores other cellular properties. For example, we know from previous studies that surface charge properties affect the DEP collection of mammalian cells below 100 Hz [4,8] but no theoretical model is currently available to incorporate this parameter. With these limitations in mind, we note that Eqn. 2 in Appendix A predicts that the cross-over frequency in the frequency range studied will depend strongly on the electrical permittivity of the membrane (ϵ_{mem}) and on its conductivity (σ_{mem}), as well as on the corresponding properties of the suspending medium (ϵ_s and σ_s). However, it should be relatively insensitive to changes in the cytoplasmic conductivity, σ_{in}, when $\sigma_{in} >> \sigma_{mem}$, and to changes in the cytoplasmic electrical permittivity, ϵ_{in}. The ion-sensitive electrodes revealed that the cells leaked as much as 50% of their intracellular K^+ into the suspending medium during the 45 min taken to complete an experiment. On the basis of the single shell model, we would expect such leakage to strongly affect the cross-over frequency by increasing the suspension conductivity. However, cytoplasmic conductivity remained sufficiently high to fulfill the conditions to prevent this from significantly affecting the cross-over frequency. For the purpose of analysis according to the predictions of the single-shell model, suspension conductivities were measured at each cross-over frequency and the cytoplasmic conductivity was calculated from the ion leakage from the cells assuming an initial cytoplasmic concentration of 150 mM. With the further assumptions that $\epsilon_{in} = 59\epsilon_0$, $\epsilon_s = 80\epsilon_0$, $d = 4.5$ nm and the cell radius was 6.25 μm for untreated cells and 5.63 μm for HMBA-treated cells (as measured by Coulter and side-scatter techniques using flow cytometry), least-squares regression analysis was performed using the Nelder-Mead simplex method [22] to find the dielectric parameters giving an optimum fit to the DEP surfaces (such as in Fig. 2).

The analyses of the surfaces yielded values for the membrane capacitance and membrane conductivity of the cells that are shown in Tables I and II. From this

TABLE I

Membrane parameters for DS19 cells derived from regression analysis of cross-over frequency data

Parameter	No treatment	HMBA	
σ_{mem}	$5.7 \cdot 10^{-7}$	$< 1 \cdot 10^{-7}$	S/m
ϵ_{mem}	6.42	4.51	
C_{mem}	1.27	0.89	$\mu F/cm^{-2}$

TABLE II

Membrane parameters for R1 cells derived from regression analysis of cross-over frequency data

Parameter	No treatment	HMBA	
σ_{mem}	$7.65 \cdot 10^{-7}$	$5.02 \cdot 10^{-7}$	S/m
ϵ_{mem}	6.91	6.77	
C_{mem}	1.34	1.30	$\mu F/cm^{-2}$

model, it is clear that HMBA induced at least a six-fold decrease in cell membrane conductivity and a decrease of approx. 30% in membrane capacitance in DS19 cells based upon the single-shell model. DMSO was found to induce similar effects. The membrane changes developed over the 4-day course of treatment with HMBA or DMSO and paralleled morphological alterations in the cells and the expression of hemoglobin as the cells differentiated.

Of particular significance with regard to the differentiation responses of the MEL cells to HMBA and DMSO was the result for R1, a murine erythroleukemia cell line cloned from DS19 that is characterized by its inability to terminally differentiate and produce hemoglobin following differentiation treatment. Table II shows that the dielectrophoretic properties of this cell line exhibited little response following exposure to these agents. Decreases in membrane capacitance and conductance, which occurred for DS19 but not for R1 following treatment by HMBA or DMSO, therefore appeared to be correlated with cell differentiation. It is especially interesting to note that the phenomenon of electrorotation, which is closely related to dielectrophoresis and yields essentially the same physical parameters [17,23], has been used to probe the membrane properties of T and B lymphocytes before and after mitotic stimulation [23]. Cell membrane capacitances were found to rise approx. 70% and membrane conductivities to increase approx. five-fold when these two cell types were stimulated from their resting states into growth [24]. It is tempting to propose that those results are a mirror image of our own if stimulation to cell division and induction to non-division can be considered converse manipulations.

While application of the single-shell model to the analysis of DEP data allows some useful comparisons to be made between the responses of different cell types to differentiation treatment, it is important to realize its limitations.

Firstly, the parameters obtained by the Nelder-Mead algorithm (Tables I and II) show that the membrane capacitance decreased by about 30% following HMBA treatment. The single-shell model envisions the membrane as a thin, homogeneous, spherical shell. In reality, the plasma membrane is now known to be inhomogeneous over its surface with respect to composition and structure and to be convoluted and invaginated. With these realities in mind, the lowering of the effective membrane capacitance following HMBA treatment can be interpreted in terms of a lessening in membrane convolution, resulting in a decrease in the area of membrane required to surround a given cell volume; an increase in the thickness of the membrane, causing a lowering of the capacitance per unit area; a reduction in charged, mobile, intramembrane components, resulting in a decrease in the electrical polarizability of the membrane, or any combination of these factors. Cell differentiation is associated with changes in the glycocalyx on the outer leaflet of the plasmalemma, with the development of cytoskeletal linkages to integrins on the inner leaflet and with alterations in the lipid and protein composition of the membrane interior. It would not be surprising if all of the suggested membrane parameters were altered following HMBA treatment. Clearly, from the point of view of developing DEP as a tool for studying cellular properties, it will be important to develop experimental and theoretical analyses that can distinguish which effect is dominant, if any.

Secondly, the conductivity intercept on the plot of cross-over frequencies (Fig. 3) occurs at 0.6 mS/m for untreated cells compared with < 0.1 mS/m for the HMBA-treated samples. In the single-shell model of the cell, this intercept is proportional to an isotropic conductivity defined for the membrane. Membrane conductivity values from Nelder-Mead minimizations of the single shell model for untreated and HMBA-treated samples are shown in Tables I and II. While many properties of the membrane are difficult to manipulate rapidly, the conductivity of the membrane can be altered by the use of an ionophore or a soap. Therefore, we tested whether manipulation of the transmembrane conductivity altered the intercept as predicted in the single-shell model by exposing HMBA-treated cells (having a low conductivity intercept) to 12 μg/ml saponin or 1 mM valinomycin, a K^+ ionophore. Effects on leakage of intracellular constituents through the membrane facilitated by various doses of saponin have been characterized previously [20], and at 12 μg/ml saponin, leakage of all ionic species was expected to occur while protein remained inside the cell. Leakage of ions from the saponized and valinomycin-treated cells, as determined by the rate of change of conductivity of the extracellular sucrose medium, was roughly doubled and tripled, respectively, compared with untreated cells. However, the cross-over frequency versus conductivity plot for treated cells was virtually identical to that of their untreated counterparts. This finding clearly shows that the intercept was not a straightforward reflection of ionic conductivity across the membrane and suggests that isotropic membrane conductivity in the single-shell model is an over-

simplification in the context of viable mammalian DS19 cells. Arnold et al. [25] analyzed electrorotation in latex particles having a conductivity component parallel to the surface, as well as a component through the particle (see also Ref. 21). Although saponin and valinomycin clearly affected the permeability of the membrane to ions, as reflected by the increased rate of ion loss from treated cells, these agents probably did not greatly affect the conductivity component parallel to the cell surface. Our results suggest that this conductivity component was significantly larger than the transmembrane component in the MEL cells and indicates that the addition of a second, more conductive shell outside the shell of the membrane may be required to take this into account.

Thirdly, the cross-over from negative to positive DEP collection that occurred at frequencies below 20 Hz is inconsistent with either single- or multi-shelled models of the cell that take into account only the capacitative and resistive properties of the cell membrane [17,21,23]. This is because dielectric systems always exhibit decreasing polarizability and increasing conductivity as the frequency rises. It follows that the observed low frequency cross-over from negative to positive DEP with decreasing frequency can only be explained by introducing a membrane parameter previously overlooked in theoretical discussions of DEP. Two possibilities for this missing parameter are membrane inductance and membrane surface charge.

Inductive properties of the cell plasma membrane were first observed by Cole and Baker [26] in measuring the longitudinal electrical impedance of the squid giant axon at frequencies below 200 Hz. This anomalous inductive reactance was later to be understood as the frequency-domain manifestation of time- and voltage-dependent K^+ redistributions in the membrane [27] characteristics as embodied in the celebrated Hodgkin-Huxley equations [28]. Such time-dependent conductance could, in principle, account for the anomalous low-frequency positive DEP observed here by causing a phase difference between the applied field and the cell membrane polarization at low frequencies. MEL cells are known to contain quinine-sensitive calcium-gated K^+ channels, Na^+ channels, and Cl^-/HCO_3^- channels [29,30]. These can be blocked with 100 μM quinine, 1 μM tetrodotoxin or 500 μM 4,4'-diisithiocyanatostilbene-2,2'-disulfonic acid (DIDS), respectively. Exposure of DS19 cells to these agents resulted in no observable changes in the anomalous low-frequency positive DEP collection, however, suggesting that inductive membrane characteristics associated with the dominant ion channels known to occur in MEL cells probably played no role in their DEP behavior below 100 Hz.

In contrast, treatment of MEL cells with neuraminidase to lower their net surface charge significantly reduced their anomalous low-frequency positive DEP collection. Reduction of net surface charge by 60%, as determined by electrophoresis [14], for example, resulted in a fall of the cross-over frequency from 20 Hz to 10 Hz coupled with a reduction of the net collection (see Fig. 4). This result strongly suggests that the anomalous DEP collection arose from cell surface charge effects not accounted for in current DEP model. Responses at frequencies above 100 Hz were not affected by neuraminidase treatment. Furthermore, this result agrees with our earlier optical absorbance measurements that showed a response of the low-frequency collection of cells to neuraminidase, implicating surface charge effects [4]. Goosens and Van Biesen [31] have described the net displacement of cells in an alternating electric field due to surface charge, and Kaler et al. have reported an anomalous low-frequency positive DEP force observed by the sensitive levitation method [7,19].

These limitations of the single-shell model suggest refinements that can be introduced and also point out important areas in which experimental methods need to be developed to probe the underlying bases for the observed DEP differences between dissimilar cell types and between undifferentiated and differentiated cells. The observed different DEP characteristics imply that there are conditions under which different cell subpopulations can be separated from each other. In Fig. 3, for example, the set of frequency/conductivity pairs bounded by the two plots corresponds to those conditions under which HMBA-treated cells exhibit negative dielectrophoresis and untreated cells exhibit positive DEP. We have demonstrated that normal erythrocytes can be separated from erythroleukemia cells [15]. These results suggest the use of DEP for cell characterizations with possible diagnostic and cell sorting implications. It is a goal of this laboratory to develop this potential usefulness of DEP as a technology for cell separation in clinical and biotechnological applications.

Finally, cells in sucrose suspensions were often observed to burst during the course of an experiment and formed spherical debris about four times the volume of unburst cells. These were clearly visible under phase-contrast microscopy. Interestingly, this spherical material could be collected by positive DEP for several minutes after the bursting event, indicating that it remained highly polarizable following destruction of the plasma membrane. The origin of this high polarizability could be containment of ions within mitochondria and other organelles or other ionic mobility effects in the cell debris.

Acknowledgements

We thank Robyn Rhea for cell preparation and Drs. Xiao-Bo Wang and Ying Huang for valuable discus-

sions. This work was supported by the National Foundation for Cancer Research and by a grant from the Advanced Technology Program of the Texas Higher Education Coordinating Board.

Appendix A

In order to fully appreciate the DEP results, it is helpful to consider the phenomenological equation describing the force, F, experienced by a particle in a non-homogeneous field, E:

$$F = 2\pi\epsilon_0\epsilon_s R^3 \mathrm{Re}\left(\frac{\zeta_p - \zeta_s}{\zeta_p + 2\zeta_s}\right)(E\cdot\nabla)E \qquad (1)$$

where $\epsilon_0 = 8.85 \cdot 10^{-12}$ F/m is the permittivity of free space, ϵ_s the relative permittivity of the suspending medium, R the cell outer radius, E the RMS electric field strength, and each $\zeta = \epsilon - j\sigma/\omega$ a complex permittivity with subscripts p and s, denoting the particle and its suspending medium, respectively [17]. The complex permittivity of the cell ζ_p is the unknown that we wish to determine. When the real part (denoted by Re) of the bracketted expression in ζ terms is positive, the force on the cells and their motion is towards regions of high E^2 and is termed positive DEP; conversely, a negative value for the real part of the ζ expression corresponds to motion away from such field regions and is termed negative DEP.

Various models have been proposed to analyze the effective cell permittivity ζ_p such as the multi-shell model derived by Irimajiri et al. [21], which considers the cell to consist of a set of homogeneous spherical shells. For our mammalian cells, this can, as a first approximation, be simplified to a single shell of radius r and permittivity $\zeta_{in} = \epsilon_{in} - j\sigma_{in}/\omega$ surrounded by a thin, homogeneous, spherical membrane of thickness d and permittivity $\zeta_{mem} = \epsilon_{mem} - j\sigma_{mem}/\omega$. [18,21]. Under these highly idealized conditions, the complex permittivity of the cell can then be written as

$$\zeta_p = \zeta_{mem}\frac{\left(\frac{r+d}{r}\right)^3 + 2\left(\frac{\zeta_{in} - \zeta_{mem}}{\zeta_{in} + 2\zeta_{mem}}\right)}{\left(\frac{r+d}{r}\right)^3 - \left(\frac{\zeta_{in} - \zeta_{mem}}{\zeta_{in} + 2\zeta_{mem}}\right)}. \qquad (2)$$

References

1 Pohl, H.A. (1978) Dielectrophoresis, Cambridge University Press, New York.

2 Price, J.A.R., Burt, J.P.H. and Pethig, R. (1988) Biochim. Biophys. Acta 964, 221–230.

3 Masuda, S., Washizu,, M. and Nanba, T. (1989) IEEE Trans. Ind. Appl. 25, 732–737.

4 Burt, J.P.H., Pethig, R., Gascoyne, P.R.C. and Becker, F.F. (1990) Biochim. Biophys. Acta 1034, 93–101.

5 Hagedorn, R., Fuhr, G., Muller, T. and Gimsa, J. (1992) Electrophoresis 13, 49–54.

6 Dimitrov, D.S. and Zhelev, D.V. (1987) Bioelectrochem. Bioenerg. 17, 549–557.

7 Kaler, K.V.I.S. and Jones, T.B. (1990) Biophys. J. 57, 173–182.

8 Pethig, R. (1990) in Automation in Biotechnology (Karube, I., ed.), pp.159–185, Elsevier, New York.

9 Singer, D. Cooper, M., Maniatis, G.M., Marks, P.A. and Rifkind, R.A. (1974) Proc. Natl. Acad. Sci. USA 71, 2668–2670.

10 Ohta, Y., Tanaka, M., Terada, M., Miller, O.J., Bank, A., Marks, P.A. and Rifkind, R.A. (1976) Proc. Natl. Acad. Sci. USA 73, 1232–1236.

11 Marks, P.A., Chen, Z.-X., Banks, J. and Rifkind, R.A. (1983) Proc. Natl. Acad. Sci. USA 80, 2282–2284.

12 Marks, P.A., Rifkind, R.A., Bank, A., Terada, M., Gambari, R., Fibachi, E., Maniatis, G. and Reuben, R. (1979) in Conference on Cellular and Molecular Regulation of Hemoglobin (Switching, G., Stamatoyannopoulos and Nienhuis, A.W., eds.), pp. 437–456, Grune and Stratton, New York.

13 Shen, G.-W., Real, F.X., DeLeo, A.B., Old, L.J., Marks, P.A. and Rifkind, R.A. (1989) Proc. Natl. Acad. Sci. USA, 80, 5919–5922.

14 Gascoyne, P.R.C. and Becker, F.F. (1990) J. Cell. Physiol. 142, 309–315.

15 Gascoyne, P.R.C., Huang, Y., Pethig, R., Vykoukal, J. and Becker, F.F. (1992) Meas. Sci. Technol. 3, 439–445.

16 Gascoyne, P.R.C., Noshari, J., Becker, F.F. and Pethig, R. (1993) IEEE Industrial Applications Society Proceedings, in press.

17 Pethig, R., Huang, Y., Wang X-B. and Burt, J.P.H. (1992) J. Phys. D: Appl. Phys. 24, 881–888.

18 Marszalek,P., Zielinski, J.J., Fikus, M. and Tsong, T.Y. (1991) Biophys. J., 59, 982–987.

19 Kaler, K.V.I.S., Xie, J-P., Jones, T.B. and Paul, R. (1992) Biophys. J. 63, 58–69.

20 Wassler, M., Jonasson, I., Persson, R. and Fries, E. (1987) Biochem. J. 247, 407–415.

21 Irimajiri, A., Hanai, T. and Inouye, A. (1979) J. Theor. Biol. 78, 251–269.

22 Dennis, J.E. and Woods, D.J. (1987) in New Computing Environments: Microcomputers in Large-Scale Computing (Wouk, A., ed.), pp. 116–122, SIAM.

23 Wang, X-B., Pethig, R. and Jones, T.B. (1992) J. Phys. D: Appl. Phys. 25, 905–912.

24 Hu, X., Arnold, W.M. and Zimmermann, U. (1990) Biochim. Biophys. Acta 1021, 191–200.

25 Arnold, W.M., Schwan, H.P. and Zimmermann, U. (1987) J. Phys. Chem. 91, 5093–5098.

26 Cole, K.S. and Baker, R.F. (1941) J. Gen. Physiol. 24, 771–788.

27 Cole, K.S. (1952) Physiol. Rev., 45, 340–379.

28 Hodgkin, A.L. and Huxley, A.F. (1952) J. Physiol. 117, 500–544.

29 Arcangeli, A., Wanke, E., Olivotto, M., Camagni, S. and Ferroni, A. (1987) Biochem. Biophys. Res. Commun. 146, 1450–1457.

30 Smith, R.L., Macara, I.G., Levenson, R., Housman, D. and Cantley, L. (1982) J. Biol. Chem. 257, 773–780.

31 Goosens, K. and Van Biesen, L. (1989) Separation Sci. Technol. 24, 51–62.